PERGAMON

International Journal of Heat and Mass Transfer 45 (2002) 4201–4216

International Journal of HEAT and MASS TRANSFER

www.elsevier.com/locate/ijhmt

# Influence of the particle–turbulence modulation modelling in the simulation of a non-isothermal gas–solid flow

P. Boulet *, S. Moissette

*LEMTA, Equipe LUMEN-ESSTIN, 2 rue Jean Lamour, 54519 Vandoeuvre les Nancy Cedex, France*

Received 28 May 2001; received in revised form 1 October 2001

**Abstract**

A gas–solid suspension upward flowing in a heated vertical pipe has been simulated numerically using both Eulerian–Eulerian and Eulerian–Lagrangian approaches. Particular attention has been paid to the influence of the modelling of the particle–turbulence interactions. A model based on a source-term formulation derived from a study by Crowe (Int. J. Multiphase Flow 26 (5) (2000) 719) allows predicting turbulence enhancement due to a strong particle influence in the core of the pipe flow. Calculations of suspension Nusselt numbers, characterizing the heat transfer between the pipe wall and the flow, have therefore been performed, with a satisfactory level of accuracy, compared with available experimental data. Some numerical difficulty remains however, especially due to the near-wall layer interactions which seem very difficult to simulate. 

## 1. Introduction

In the frame of multiphase flow predictions, simulation of the interphase exchanges is obviously of major interest, but unfortunately also one of the most complicated topics to be dealt with. In the study by Elghobashi [1] a map giving the importance of the interphase phenomena is plotted as a function of the particle Stokes number and the loading ratio. Particles are described to have a negligible effect on the turbulence at very low volume fractions (lower than $10^{-6}$). On the contrary, they may enhance or reduce the turbulence for higher values, depending on their Stokes number. For values of the volume fraction between $10^{-6}$ and $10^{-3}$, this effect must be taken into account and is referred to as two-way coupling. For even higher volume fractions, the suspension is so dense that interparticle interactions also have to be taken into account, a situation which is called the four-way coupling problem. In a complementary way, one may also refer to the study presented by Gore and Crowe [2], devoted to the modulation of the turbulence due to the particles. The change in turbulence intensity is plotted as a function of the ratio between the particle diameter and a turbulent length scale (a characteristic length of the most energetic eddies). Based on the numerous experimental data available in the literature, the corresponding analysis shows an obvious trend: small particles (for which the above-defined ratio is lower than 0.1) tend to decrease the turbulence, whereas large particles tend to enhance it. Two-way and four-way coupling effects may therefore be predicted on the basis of these studies. However, prediction of the magnitude of the expected change in turbulence intensity requires complete modelling with a complex numerical solution. This topic has been addressed in numerous studies and the most classical formulation of the interphase exchanges will be discussed hereafter.

Our analysis concerns non-isothermal gas–solid flows where heat transfer is due to convection. As turbulence is known to have a strong effect on the heat transfer, an accurate model for the dynamics has to be developed, where the modulation of the flow due to the particles has to be carefully simulated. This is the purpose of the present paper, the analysis being restricted to the case where the simulation of the fluid phase is performed thanks to an Eulerian formulation based on a Reynolds averaged Navier Stokes equation (RANS)-type model,

* Corresponding author. Tel.: +33-383-685-081; fax: +33-383-685-085.

*E-mail address:* boulet@esstin.uhp-nancy.fr (P. Boulet).

0017-9310/02/$ - see front matter 
PII: S0017-9310(02)00126-6

**Nomenclature**

| | |
|---|---|
| $C_D$ | drag coefficient (dimensionless) |
| $c_p$ | specific heat (J/kg/K) |
| $d_p$ | particle diameter (m) |
| $g$ | gravitational acceleration (m/s$^2$) |
| $h_s$ | suspension heat transfer coefficient (W/m$^2$/K) |
| $h_p$ | heat transfer coefficient around particles (W/m$^2$/K) |
| $k$ | turbulent kinetic energy (m$^2$/s$^2$) |
| $l_h$ | hybrid dissipation length scale |
| $l_i$ | dissipation length scale in the pure gas case |
| $m$ | solid loading ratio (dimensionless) |
| $n$ | particle number density (m$^{-3}$) |
| $Nu_s$ | suspension Nusselt number (dimensionless) |
| $Nu_0$ | pure air Nusselt number (dimensionless) |
| $Pr$ | Prandtl number (dimensionless) |
| $q_m$ | mass flow rate (kg/s) |
| $Q_w$ | wall heat flux (W/m$^2$) |
| $r$ | radial co-ordinate (m) |
| $R$ | pipe radius (m) |
| $S_{kf}$ | turbulent kinetic energy source (kg/m/s$^3$) |
| $S_{\varepsilon f}$ | dissipation rate source (kg/m/s$^4$) |
| $S_{u_i}$ | momentum source (N/m$^3$) |
| $S_\theta$ | heat source (W/m$^3$) |
| $u_i$ | velocity component (m/s) |
| $z$ | axial co-ordinate (m) |

*Greek symbols*

| | |
|---|---|
| $\alpha$ | solid volume fraction (dimensionless) |
| $\varepsilon$ | dissipation rate of turbulent kinetic energy (m$^2$/s$^3$) |
| $\theta$ | temperature (K) |
| $\theta_m$ | bulk average temperature (K) |
| $\lambda$ | inteparticle spacing (m) |
| $\lambda_f$ | fluid thermal conductivity (W/mK) |
| $\nu_t$ | eddy viscosity (m$^2$/s) |
| $\rho$ | density (kg/m$^3$) |
| $\tau_p$ | particle relaxation time (s) |

*Subscripts and superscripts*

| | |
|---|---|
| f | fluid property |
| p | particle property |
| t | turbulent quantity |
| w | property at the wall |
| $\langle x \rangle$ | averaged quantity |
| $x'$ | fluctuating quantity |
| $\vec{x}$ | vector |

namely a non-linear low Reynolds $k$–$\varepsilon$ model in order to account for turbulence anisotropy and to improve the accuracy in the near-wall region.

In a multiphase flow, source terms are involved in order to simulate the momentum and heat exchanges between the phases. The formulation of these terms is well known and various effects, for example associated with the drag force and the lift force on one hand, or to the heat transfer by convection on the other hand, are well taken into account. In the frame of turbulent flows however, the formulation of the source terms associated with the various existing closure schemes is sometimes far from fully satisfactory. In the available models the starting-point of the analysis is always the momentum balance which is further manipulated in order to yield a complete closure scheme including the dispersed phase influence. Let us examine some of the most classical formulations. Berlemont et al. [3] and Desjonqueres [4] have presented a derivation starting from the instantaneous momentum balance, which is multiplied by the instantaneous velocity. Then Reynolds averaging is performed and the averaged mechanical energy balance is subtracted, in order to yield an averaged equation for the turbulent kinetic energy. This model has been widely used especially in Eulerian–Lagrangian formulations, but equivalent formulations have been used in two-fluid models. In particular Louge et al. [5] or He and Simonin [6] have derived complete equations adapted to the two-way coupling problem. The derivation of the turbulent intensity equation is similar to the one adopted in the frame of one-phase flows: the instantaneous momentum balance for a component of the fluid velocity $u_{f_i}$ is multiplied by the fluctuating velocity component $u'_{f_j}$, then averaging is performed. The same operation is done on the balance for $u_{f_j}$ multiplied by $u'_{f_i}$, a summation and some manipulations finally yielding the Reynolds stresses from which the turbulent kinetic energy is derived. Starting with the exact momentum balance derived in the case of a two-phase flow, this gives a closure scheme for a turbulent two-phase flow. The formulation of the source term due to the particles is finally often modelled to obtain expressions equivalent to the one used in the Eulerian–Lagrangian models.

Let us introduce some of the variables that will be further defined later in the paper: $S_{kf}$, $\alpha$, $\rho_p$, $\tau_p$, $u'_{f_i}$ and $u'_{p_i}$ respectively stand for the source of fluid turbulent kinetic energy, the volume fraction, the density of the particles, the particle characteristic time and the fluctuating velocity components for the fluid and the particles. In all previously discussed models the source term which is finally derived has a form similar to the following:

$$S_{kf} = \frac{\alpha \rho_p}{\tau_p}\left(-\langle u'_{f_i} u'_{f_i}\rangle + \langle u'_{p_i} u'_{f_i}\rangle\right) \tag{1}$$

Owing to the fact that the correlation between the fluid and the particle velocity has been demonstrated to be smaller than the fluid velocity correlation, the result for $S_{kf}$ is negative. The major drawback of these models is therefore that the obtained form of the source term can only predict a reduction of the turbulence, whereas large particles are known to be able to enhance the turbulence. The severity of this comment may be tempered taking into account some refinements that have been introduced, by He and Simonin [6] for example. Their analytical derivation of $S_{kf}$ gives the above equation with an additional term coming from the expression of the work due to the forces applied upon the particles by the turbulent eddies, in the frame of the method described above. Modelled on the basis of a drift velocity formulation and finally as a function of the gradient of the volume fraction, the contribution of this additional term has been found to be relatively small in the case of large particles and may not explain a strong increase in the turbulence due to the particles, however. In the numerical studies devoted to turbulence modulation, some attempts have been reported on the capacity of their model to predict correct turbulence profiles even for relatively large particles, despite the formulation of the source term. This may be explained considering that the production term may have a strong influence on the turbulent kinetic energy profile. When expressed as a function of the velocity gradient (as in the $k$–$\varepsilon$ model) and since the velocity profile of the fluid is affected by the particles, this production term may furnish an indirect influence of the dispersed phase on the fluid turbulence. Hence, the source term $S_{kf}$ itself does not necessarily explain alone the observed modulation.

Specific studies have been reported concerning supplementary modelling for the turbulence modulation due to the particles. In particular Yuan and Michaelides [7] have detailed the various contributions of the dispersed phase to the turbulence modification, identifying two predominant mechanisms: an extra-dissipation due to the acceleration of particles by eddies and an extra-production due to the wake of the particles. The latter effect has been invoked as a major cause capable of explaining the turbulence enhancement due to large particles. Hence several studies have been devoted to the modelling of an additional term taking into account this wake effect. Yuan and Michaelides [7] and Yarin and Hetsroni [8] in particular have succeeded in predicting some turbulent intensity changes. Such an analysis cannot be simply introduced in a conventional closure model for the turbulence however. Since a complete description of the suspension relies on the solution of a complete system for the mass, momentum and energy balances supplemented by closure equations for the turbulence, additional efforts have to be taken into account to provide a complete and accurate formulation for the above defined term $S_{kf}$, keeping in mind this wake effect.

Recently, a source term formulation featuring the particle–turbulence interaction has been derived in a more rigorous way by Crowe [9]. His analysis is that the usual formulation suffers from the fact that the conventional modelling for the forces acting on the particles provides an averaged value that is then treated like a local one. He therefore re-derived the complete formulation starting with an initial mechanical energy, where the forces acting on the particle are not modelled as equivalent point forces. On the contrary, an exact description of the exchanges taking into account the real interfacial area is performed, on the basis of a former analysis reported in [10]. After Reynolds decomposition and averaging, the averaged mechanical energy is subtracted, finally producing a complete equation for the turbulent kinetic energy. In the obtained equation, a source term may be identified, which is different from the previous Eq. (1). Keeping the same notation as in relation (1), this gives:

$$S_{kf} = \frac{\alpha\rho_p}{\tau_p}\left(|\langle u_f\rangle - \langle u_p\rangle|^2 + \left(\langle u'_{p_i}u'_{p_i}\rangle - \langle u'_{f_i}u'_{p_i}\rangle\right)\right) \tag{2}$$

Two contributions may be identified in this source term: generation by the particle drag and a transfer of kinetic energy of the particle motion to kinetic energy of the carrier fluid. In particular the term due to the work by the drag force is always positive and can have a high magnitude, avoiding the drawback discussed above for $S_{kf}$. As pointed out by Crowe, similar formulations have been presented before by others. In particular Hwang and Shen [11] started from the instantaneous total energy balance, then applied Reynolds decomposition and averaging, and finally subtracted the averaged momentum balance and the averaged thermal energy balance to write a turbulent kinetic energy equation. One may notice that in their analysis the interphase momentum exchange is not restricted only to the drag force, contrary to the study by Crowe. When only the drag force is taken into account however the derived form for the particle–turbulence interaction is the same as the one by Crowe. The phase interaction term is therefore observed to be positive, inducing turbulent enhancement which is attributed to the wake effect caused by particles.

Finally, the work of Kataoka and Serizawa [12] and Liljegren [13] have also been cited by Crowe as leading to the same formulation, since their formulation of the interfacial transport terms, which are involved in the derived equation for the turbulence of two-phase mixtures, are similar to the source term presented by Crowe.

All these studies are concerned with the turbulent kinetic energy formulation, and applying the results would be useful for the simulation of particle–turbulence interactions, but additional information is required for the turbulence dissipation rate which is involved in the

closure of the problem. Taking into account the effect of the above-mentioned production in the particle wakes, implies a requirement for an extra-dissipation term. In the classical formulation of the dissipation rate equation, an extension of the pure gas case is written. All the classical modelled terms in the one-phase case still appear in the two-phase flow model, the balance being modified introducing the volume fraction influence and adding an extra-dissipation term, which has to be associated with the extra-production of turbulent kinetic energy. The most classical formulation assumes proportionality between extra-production and extra-dissipation introducing a constant often called $C_{\varepsilon 3}$, for which various values have been proposed, that should in fact depend on the particle type and the loading ratio. One may still try to apply such a model for the dissipation balance even if the analysis applied for the turbulent kinetic energy derivation has changed. The different formulation of the extra-production term would actually imply a different value for $C_{\varepsilon 3}$, that could be computed after numerical optimisation. Lain et al. [14] recently tested this method in the case of a bubble column, succeeding in the prediction of bubble-induced turbulence phenomena. Crowe [9] has proposed an alternative method where the dissipation is estimated rather than deduced from a rigorous balance. The value obtained in the pure gas case is just altered by the introduction of a new dissipation length that takes into account a characteristic length scale of the turbulence without particles and the interparticle spacing. This yields a very simple formulation, easy to compute, that should be tested in real two-phase flow applications. A complete derivation of the dissipation rate equation would be more accurate but is still required, despite some attempts which have been reported, see Kataoka and Serizawa [12] for example.

One may finally ask if the above-discussed formulations will lead to significant progress when applied to real applications involving two-way coupling effects. This is what this paper focuses on, presenting a complete simulation of a gas–particle flow subjected to wall heat exchange and an analysis of the numerical result sensitivity to the source term formulation, in particular as concerns the turbulence source term. The usual model for the source term for the turbulent kinetic energy, involving the form presented in Eq. (1) and its current form for the dissipation has been referred to as the "classical form" in the paper. Numerical calculations performed with this model have been compared to results obtained using the formulation presented by Crowe. Both Eulerian–Eulerian and Eulerian–Lagrangian solutions are addressed. They are based on previous studies carried out by the present authors ([15,16]). The present study involves refined models however, in so far as emphasis is put on the turbulence source terms and a non-linear low Reynolds turbulence model has been introduced. The next paragraph is devoted to the complete presentation of the set of equations that has to be solved. Then some details are given on the numerical processing that has been adopted. Finally numerical results will be analysed.

## 2. Formulation

The case of a suspension flowing in a vertical heated pipe is addressed. Owing to the loading ratios considered in the numerical simulation described below, the so-called four-way coupling phenomena must be taken into account. Consequently, the present simulation involves source terms which represent the gas–particle interactions, and additional models which allow particle–particle interactions to be taken into account. One may note that volume fractions are high enough to require collision treatments in the dispersed phase modelling, whereas heat transfer by conduction always remains negligible, since the present applications concern moderately dense suspensions, but far from packed or fluidised beds however. According to Sun and Chen [17], the contact area and the impact duration are too small to induce an important heat exchange.

### 2.1. Continuous phase simulation

The continuous phase may be accurately simulated using an Eulerian formulation. A classical RANS model is applied in the present simulation, as described below. Considering the above-cited assumptions, the following equations have to be solved:

- Continuity equation:

$$\frac{\partial}{\partial x_i}((1-\alpha)\langle u_{\mathrm{f}_i}\rangle) = 0 \tag{3}$$

- Momentum equation:

$$\begin{aligned}\frac{\partial}{\partial x_j}&((1-\alpha)\rho_{\mathrm{f}}\langle u_{\mathrm{f}_i}\rangle\langle u_{\mathrm{f}_j}\rangle)\\ &= -(1-\alpha)\frac{\partial\langle P\rangle}{\partial x_i} + \frac{\partial}{\partial x_j}\left[(1-\alpha)\mu_{\mathrm{f}}\left(\frac{\partial\langle u_{\mathrm{f}_i}\rangle}{\partial x_j}+\frac{\partial\langle u_{\mathrm{f}_j}\rangle}{\partial x_i}\right)\right]\\ &\quad -\frac{2}{3}\frac{\partial}{\partial x_i}\left[(1-\alpha)\mu_{\mathrm{f}}\left(\frac{\partial\langle u_{\mathrm{f}_j}\rangle}{\partial x_j}\right)\right]\\ &\quad -\frac{\partial}{\partial x_j}((1-\alpha)\rho_{\mathrm{f}}\langle u'_{\mathrm{f}_i}u'_{\mathrm{f}_j}\rangle) + (1-\alpha)\rho_{\mathrm{f}}g_i + \langle S_{\mathrm{u}_i}\rangle\end{aligned} \tag{4}$$

- Energy equation:

$$\begin{aligned}\frac{\partial}{\partial x_j}&((1-\alpha)\rho_{\mathrm{f}}c_{\mathrm{pf}}\langle u_{\mathrm{f}_j}\rangle\langle\theta_{\mathrm{f}}\rangle)\\ &= \frac{\partial}{\partial x_j}\left[(1-\alpha)\left(\lambda_{\mathrm{f}}\frac{\partial\theta_{\mathrm{f}}}{\partial x_j} - \rho_{\mathrm{f}}c_{\mathrm{pf}}\langle u'_{\mathrm{f}_j}\theta'_{\mathrm{f}}\rangle\right)\right] + \langle S_\theta\rangle\end{aligned} \tag{5}$$

In these equations, $\alpha$ is the solid volume fraction in the flow; $P$ and $g$ stand for the pressure and the gravita-

tional acceleration; $\rho_f$, $\mu_f$, $c_{pf}$ and $\lambda_f$ are the fluid phase density, dynamic viscosity, heat capacity and thermal conductivity respectively; $u_{f_i}$ and $\theta_f$ stand for the fluid velocity components and the temperature. Angular brackets denote phase average quantities, whereas primes denote fluctuating quantities. $S_{u_i}$ and $S_\theta$ stand for the source terms due to particle-to-fluid momentum and heat transfer.

The closure problem, i.e. the expression of the mean fluctuation products, is addressed using a non-linear eddy viscosity model (NEVM) for the dynamic part of the problem associated with the generalised gradient diffusion hypothesis (GGDH) model as concerns the energy equation, as presented by Rokni and Sunden [18] for a pure fluid flow. This implies the numerical simulation of the following formulation for the Reynolds Stresses:

$$\begin{aligned}\langle u'_{f_i}u'_{f_j}\rangle &= \frac{2}{3}k_f\delta_{ij} - 2\nu_{tf}\langle S_{ij}\rangle - 4C_D C_\mu \nu_{tf}\frac{k_f}{\varepsilon_f}\\ &\quad\times\left(\langle S_{ik}\rangle\langle S_{kj}\rangle - \frac{1}{3}\langle S_{mn}\rangle\langle S_{nm}\rangle\delta_{ij}\right)\\ &\quad - 4C_E C_\mu \nu_{tf}\frac{k_f}{\varepsilon_f}\left(\langle \dot{S}_{ij}\rangle - \frac{1}{3}\langle \dot{S}_{mm}\rangle\delta_{ij}\right)\end{aligned} \tag{6}$$

where by definition $k_f = \frac{1}{2}\langle u'_{f_i}u'_{f_i}\rangle$ stands for the turbulent kinetic energy of the fluid, $\varepsilon_f$ denotes its dissipation rate and $\nu_{tf}$ stands for the eddy diffusivity of the fluid deduced from

$$\nu_{tf} = C_\mu f_\mu \frac{k_f^2}{\varepsilon_f} \tag{7}$$

Moreover, $\langle S_{ij}\rangle = \frac{1}{2}\left(\frac{\partial\langle u_{f_i}\rangle}{\partial x_j} + \frac{\partial\langle u_{f_j}\rangle}{\partial x_i}\right)$

and

$$\langle \dot{S}_{ij}\rangle = \frac{1}{2}\left(\langle u_{f_k}\rangle\frac{\partial\langle S_{ij}\rangle}{\partial x_k} - \frac{\partial\langle u_{f_i}\rangle}{\partial x_k}\langle S_{kj}\rangle - \frac{\partial\langle u_{f_j}\rangle}{\partial x_k}\langle S_{ki}\rangle\right) \tag{8}$$

Such a NEVM formulation has been chosen since it provides an explicit and efficient way to obtain information on the Reynolds stresses. Little computational effort is therefore required to extend the capability of a classical $k$–$\varepsilon$ model, as compared to the complexity required by a complete second order closure (like the so-called RSM model). Despite this simplicity, it allows the anisotropy of the turbulence to be taken into account. Consequently, comparisons with experimental data like streamwise components of the fluctuating velocity will be done using a true calculated $u'_f$ instead of an estimated value based on $\sqrt{2k_f/3}$, as is usually done when using a basic $k$–$\varepsilon$ model. Moreover the Reynolds stresses will also be useful when dealing with the dispersion problem in the simulation of particle motion using a Lagrangian tracking code.

To make the formulation complete the turbulent heat fluxes are modelled in such a way that

$$\langle u'_{f_j}\theta'_f\rangle = -C_t f_{\mu t}\frac{k_f}{\varepsilon_f}\left(\langle u'_{f_i}u'_{f_k}\rangle\frac{\partial\langle\theta_f\rangle}{\partial x_k}\right) \tag{9}$$

Additional balance equations have therefore to be written for $k_f$ and $\varepsilon_f$:

$$\begin{aligned}(1-\alpha)\rho_f\langle u_{f_j}\rangle\frac{\partial k_f}{\partial x_j} &= -\frac{\partial}{\partial x_j}\left[(1-\alpha)\rho_f\left(\nu_f + \frac{\nu_{tf}}{\sigma_k}\right)\frac{\partial k_f}{\partial x_j}\right]\\ &\quad - (1-\alpha)\rho_f\langle u'_{f_i}u'_{f_j}\rangle\frac{\partial\langle u_{f_i}\rangle}{\partial x_j}\\ &\quad - (1-\alpha)\rho_f\varepsilon_f + S_{kf}\end{aligned} \tag{10}$$

and

$$\begin{aligned}(1-\alpha)\rho_f\langle u_{f_j}\rangle\frac{\partial\varepsilon_f}{\partial x_j} &= -\frac{\partial}{\partial x_j}\left[(1-\alpha)\rho_f\left(\nu_f + \frac{\nu_{tf}}{\sigma_\varepsilon}\right)\frac{\partial\varepsilon_f}{\partial x_j}\right]\\ &\quad - (1-\alpha)\rho_f\frac{\varepsilon_f}{k_f^2}\left[C_{\varepsilon1}f_1\langle u'_{f_i}u'_{f_j}\rangle\frac{\partial\langle u_{f_i}\rangle}{\partial x_j}\right.\\ &\quad \left. + C_{\varepsilon2}f_2\varepsilon_f\right] + S_{\varepsilon f}\end{aligned} \tag{11}$$

where $S_{kf}$ and $S_{\varepsilon f}$ are supplementary source terms due to the influence of the particles.

All constants $C_D$, $C_E$, $\sigma_k$, $\sigma_\varepsilon$, $C_{\varepsilon1}$, $C_{\varepsilon2}$ and $C_\mu$ and damping functions $f_1$, $f_2$, $f_\mu$ and $f_{\mu t}$ have been based on values generally used for one-phase flows. In particular, the values prescribed in the low-Reynolds $k$–$\varepsilon$ model proposed by Myong and Kasagi [19] have been chosen and associated with complementary expressions given by Rokni and Sunden [18] concerning the specific data associated with the NEVM and GGDH models. All details are given in Table 1. This particular choice was done in order to combine the benefits of two models: (i) the

Table 1
Constants and damping functions used in the model

| $C_D$ | $C_E$ | $\sigma_k$ | $\sigma_\varepsilon$ | $C_{\varepsilon1}$ | $C_{\varepsilon2}$ | $C_\mu$ | $C_t$ | $f_1$ |
|---|---|---|---|---|---|---|---|---|
| 1.68 | 1.68 | 1.4 | 1.3 | 1.4 | 1.8 | 0.09 | 0.25 | 1.0 |

| $f_2$ | $f_\mu$ | $f_{\mu t}$ |
|---|---|---|
| $\left[1-\frac{2}{9}\exp\left(\left(\frac{Re_t}{6}\right)^2\right)\right]\left(1-\exp\left(\frac{-y^+}{5}\right)\right)^2$ | $\left[1+\frac{3.45}{\sqrt{Re_t}}\right]\left(1-\exp\left(\frac{-y^+}{70}\right)\right)$ | $\left[(1-\exp(-0.0225Re_k))^2\right]\left(1+\frac{41}{Re_t}\right)$ |
| with $Re_t = k_f^2/\nu_f\varepsilon_f$ | | with $Re_k = \sqrt{k_f}d/\nu_f$ |

accuracy of Myong and Kasagi' low-Reynolds model, which has been compared with other models and finally prescribed in the case of a pipe flow by Hrenya et al. [20,21]; (ii) the care brought to the model presented by Rokni and Sunden [18] as concerns the effect of turbulence anisotropy and the turbulent heat flux description. Instead of the value $C_t = 0.3$ which was suggested by Rokni and Gatski [22], a slightly different value has been used here, namely $C_t = 0.25$ , which has been found to produce the best results in our case of a cylindrical duct when compared with available correlations used in the pure gas case. Some of these coefficients ($\sigma_k$, $\sigma_\varepsilon$, $C_{\varepsilon 1}$, $C_{\varepsilon 2}$ and $C_\mu$) have been tested by Bolio et al. [23] showing only a weak effect on the final results upon slightly varying the coefficients ($\pm 0.1$) from the original values given by Myong and Kasagi. In particular, only the peak intensity of the $k_f$ prediction was observed to be influenced by variations in $C_{\varepsilon 1}$ and $C_{\varepsilon 2}$.

The various source terms which are involved in the above set of equations are due to well-identified physical phenomena. Owing to the special gas–solid flow which is of interest in the present study, the following effects may be identified:

(i) $S_{u_i}$ stands for the momentum exchange due to forces acting on the particles (drag and lift force);
(ii) $S_\theta$ stands for the heat exchange between the two phases (radiative transfer and conduction during collisions being neglected, this term is entirely due to the convection phenomena around the particles);
(iii) $S_{kf}$ stands for the extra-production of fluid turbulent kinetic energy due to the particles (as discussed in the introduction and detailed in Table 2)
(iv) $S_{\varepsilon f}$ is the corresponding extra-dissipation term.

Besides the model which is adopted for these source terms, the numerical computation also depends on the approach adopted for the dispersed phase simulation. Two classical particle phase descriptions and their corresponding source term simulations are described in the following paragraph.

### 2.2. Dispersed phase simulation

Lagrangian tracking and Eulerian simulation are two usual ways of simulation, suitable for the dispersed phase modelling and widely reported in the literature. Both have been tested in the present study.

- In the case where an *Eulerian simulation* is used, the dispersed phase is represented as a continuum. A set of equations has therefore to be written as has been reported in Boulet et al. [15]. In the present study, the following balance equations were solved:
  - Continuity equation:

$$\frac{\partial}{\partial x_i}(\alpha\langle u_{p_i}\rangle) = 0 \tag{12}$$

  - Momentum equation:

$$\frac{\partial}{\partial x_j}(\alpha\rho_p\langle u_{p_i}\rangle\langle u_{p_j}\rangle) = -\frac{\partial}{\partial x_j}(\alpha\rho_p\langle u'_{p_i}u'_{p_j}\rangle) + \alpha\rho_p g_i - \langle S_{u_i}\rangle \tag{13}$$

  - Energy equation:

$$\frac{\partial}{\partial x_j}(\alpha\rho_p c_{pp}\langle u_{p_j}\rangle\langle\theta_p\rangle) = -\frac{\partial}{\partial x_j}[\alpha(\rho_p c_{pp}\langle u'_{p_j}\theta'_p\rangle)] - \langle S_\theta\rangle \tag{14}$$

Table 2
Source term formulation

| Source term | Eulerian–Eulerian formulation | Eulerian–Lagrangian formulation |
|---|---|---|
| $\langle S_{u_i}\rangle$ | $\frac{\alpha\rho_p}{\tau_p}(\langle u_{p_i} - u_{f_i}\rangle)$ | $n\left\langle -m_p\left(\frac{du_{p_i}}{dt} - g_i\right)\right\rangle$ |
| $\langle S_\theta\rangle$ | $\frac{6\alpha h_p}{d_p}(\langle\theta_p - \theta_f\rangle)$ | $n\langle h_p\pi d_p^2(\theta_p - \theta_f)\rangle$ |
| $S_{kf}$ in model 1 (classical form) | $\frac{\alpha\rho_p}{\tau_p}(-\langle u'_{f_i}u'_{f_i}\rangle + \langle u'_{p_i}u'_{f_i}\rangle)$ | $\langle S'_{u_i}u'_{f_i}\rangle$ |
| $S_{\varepsilon f}$ in model 1 (classical form) | $C_{\varepsilon 3}(\varepsilon_f/k_f)S_{kf}$ with $C_{\varepsilon 3}$ ranging from 1.1 to 1.9 according to the literature—a value of 1.8 has been used in the present paper, except in some particular specified cases | |
| $S_{kf}$ in model 2 (derived from the model by Crowe [9]) | $\frac{\alpha\rho_p}{\tau_p}(\lvert\langle u_f\rangle - \langle u_p\rangle\rvert^2 + (k_p - k_{fp}))$ | $\lvert\langle S_{u_i}\rangle\langle u_{f_i} - u_{p_i}\rangle\rvert + \langle S'_{u_i}u'_{p_i}\rangle$ |
| Specific equation for $\varepsilon_f$ in model 2 (as derived by Crowe [9]) | $\varepsilon_f = \frac{k_f^{3/2}}{l_h}$ | |
| $S_{kf}$ and $S_{\varepsilon f}$ in model 3 (test of an hybrid formulation) | The same form is kept for $S_{kf}$ as in model 2 and the dissipation is sought as the solution of a classical balance, as in model 1 | |

Again, closure equations must be added to allow solution of the whole problem. The model by He and Simonin [6] was applied here. Equations are given for the completeness of the description of our simulation conditions, but the reader is referred to the cited reference for the details of the derivation.

- Balance for the kinetic energy of the dispersed phase ($k_p$):

$$\alpha\rho_p\langle u_{p_j}\rangle\frac{\partial k_p}{\partial x_j}=\frac{\partial}{\partial x_j}\left[\alpha\rho_p K_{tp}\frac{\partial k_p}{\partial x_j}\right]-\alpha\rho_p\langle u'_{p_i}u'_{p_j}\rangle\frac{\partial\langle u_{p_i}\rangle}{\partial x_j}-S_{cp}+S_{kp} \quad (15)$$

where the various involved parameters are the followings:

(i) The dispersed phase eddy diffusivity:

$$K_{tp}=\left(\frac{\tau_t k_{fp}}{1.84}+\frac{\tau_p k_p}{2.7}\right)\left(1+\frac{\tau_p\xi_c}{1.8\tau_c}\right)^{-1}$$

involving the interparticle collision coefficient $\xi_c=(1+e_c)(49-33e_c)/100$ ($e_c$ designating the interparticle restitution coefficient) and the average time between interparticle collisions, which may be calculated as: $\tau_c=d_p/(24\alpha\sqrt{\pi}\sqrt{2k_p/3})$;

(ii) The dispersed phase kinetic stresses based on an eddy viscosity concept ($\nu_{tp}$) which leads to:

$$\langle u'_{p_i}u'_{p_j}\rangle=-\nu_{tp}\left(\frac{\partial\langle u_{p_i}\rangle}{\partial x_j}+\frac{\partial\langle u_{p_j}\rangle}{\partial x_i}\right)+\frac{2}{3}\delta_{ij}\left(k_p+\nu_{tp}\frac{\partial\langle u_{pm}\rangle}{\partial x_m}\right)$$

where

$$\nu_{tp}=\left(\nu_{tfp}+\frac{\tau_p k_p}{3}\right)\left(1+\frac{\tau_p\sigma_c}{2\tau_c}\right)^{-1}$$

($\sigma_c=0.2(1+e_c)(3-e_c)$ being a second interparticle coefficient and $\nu_{tfp}$ a fluid–particle eddy viscosity as defined below);

(iii) The source term due to collisions: $S_{cp}=\alpha(1-e_c^2)(k_p/3\tau_c)$;

(iv) The source term due to interphase exchanges: $S_{kp}=(\alpha/\tau_p)(-2k_p+k_{fp})$.

- Balance for the particle–fluid covariance defined by the trace of the covariance matrix of the particle and fluid fluctuating velocity vectors ($k_{fp}$):

$$\alpha\rho_p\langle u_{p_j}\rangle\frac{\partial k_{fp}}{\partial x_j}=\frac{\partial}{\partial x_j}\left[\alpha\rho_p\nu_{tfp}\frac{\partial k_{fp}}{\partial x_j}\right]-\alpha\rho_p\langle u'_{f_i}u'_{p_j}\rangle\frac{\partial\langle u_{p_i}\rangle}{\partial x_j}-\alpha\rho_p\langle u'_{f_j}u'_{p_i}\rangle\frac{\partial\langle u_{f_i}\rangle}{\partial x_j}-\alpha\rho_p\frac{k_{fp}}{\tau_t}+S_{k_{fp}} \quad (16)$$

where the following models are used:

(i) The fluid–particle eddy viscosity is $\nu_{tfp}=(1/3)k_{fp}\tau_t$, where $\tau_t$ denotes a characteristic time for particle–turbulence interaction:

$$\tau_t=\frac{\nu_{tf}}{(2/3)k_f}\left(1+0.45\frac{(|\vec{u}_f-\vec{u}_p|)^2}{(2/3)k_f}\right)^{-1/2}$$

(ii)

$$\langle u'_{f_i}u'_{p_j}\rangle=-\nu_{tfp}\left(\frac{\partial\langle u_{f_i}\rangle}{\partial x_j}+\frac{\partial\langle u_{p_j}\rangle}{\partial x_i}\right)+\frac{1}{3}\delta_{ij}\left(k_{fp}+\nu_{tfp}\frac{\partial\langle u_{fm}\rangle}{\partial x_m}+\nu_{tfp}\frac{\partial\langle u_{pm}\rangle}{\partial x_m}\right)$$

(iii) $\alpha\rho_p(k_{fp}/\tau_t)$ stands for the dissipation of the particle–fluid covariance due to fluid viscosity and decorrelation between the fluctuations of both phases;

(iv) Finally, the last term stands for the interaction between the fluctuations of both phases:

$$S_{k_{fp}}=-\frac{\alpha\rho_p}{\tau_p}[(1+X)k_{fp}-k_f-Xk_p]$$

where $X=(\alpha\rho_p/((1-\alpha)\rho_f)$

As can be seen, various influences on the dispersed phase may be taken into account: namely the drag force, gravity, the fluid turbulence action, the collision effects and the heat transfer by convection around the particles. Additional forces like the lift force are not, however, included in the formulation.

Boundary conditions are written as in [6] allowing inelastic collisions to be taken into account. Additional conditions are written for the dispersed phase temperature: fixed temperature at the entry of the heated zone, symmetry condition on the pipe axis and $d\langle\theta_p\rangle/dr=0$ at the pipe wall: (conduction between the wall and the particles being negligible).

- On the contrary, *Lagrangian simulations* are based on the tracking of individual particles suspended in the fluid flow. Various effects undergone by the particles may be accurately taken into account. Details concerning the effects listed below and the way they have been taken into account may be found in Boulet et al. [16]. In the present study, special care has been taken concerning:

(i) The forces acting on particles: gravity, drag force and lift force due to rotation (only the case of massive particles has been addressed here, involving strong rotational velocities; shear lift force was not taken into account at present, owing to the lack of accurate information about its modelling, in particular when dealing with massive particles with a particle Reynolds number far above 1);

(ii) Wall–particle collisions (a virtual wall model as presented and validated by Sommerfeld [24] is applied);
(iii) Particle–particle collisions (a probabilistic model is used, where the computed collision frequency is based on a formulation in agreement with $\tau_c$ (the average time between interparticle collisions used in the Eulerian–Eulerian formulation), thus allowing comparisons between the two approaches);
(iv) Particle–turbulence model (a recent dispersion model tested by Moissette et al. [25] has been applied).

Computational details concerning the numerical process are given later.

### 2.3. Source term formulation

This topic is one of the main interests of the present work. Following the available literature, several methods have been applied to deal with this problem.

Table 2 summarises the way the various source terms have been calculated, depending on the numerical scheme adopted for the complete simulation. Note that in the original formulation by Crowe, the dissipation $\varepsilon_f$ is simply deduced from the value computed in the pure fluid case, modified by introducing a so-called hybrid length scale (written $l_h$) based on the interparticle spacing ($\lambda$) and the initial dissipation length scale ($l_i$) as used in single phase flows. Following Crowe [9], this yields the equation given in Table 2 for $\varepsilon_f$ where $l_h$ is such that

$$\frac{1}{l_h}=\frac{1}{l_i}+\frac{1}{\lambda} \quad \text{with} \quad \lambda = d_p\left[\left(\frac{\pi}{6\alpha}\right)^{1/3}-1\right] \tag{17}$$

In the following, calculations obtained applying the classical form of the source terms $S_{kf}$ and $S_{\varepsilon f}$, are referred to as *model 1*. The formulation given by Crowe [9] (with the corresponding $S_{kf}$ and the original formulation of the dissipation, based on the length scale given by relation (17)) is referred to as *model 2*. Particular computations, referred to as *model 0*, have also been carried out using a one-way coupling scheme, in order to present numerical reference data for further comparisons.

## 3. Numerical study

In order to test the numerical simulation presented in the previous paragraph, computations have been performed for a non-isothermal gas–solid suspension turbulently upward flowing in a vertical pipe. The following assumptions have been made:

- the flow is dynamically fully developed but entering in a heated area, being therefore a thermally developing flow;
- particles are perfectly spherical, each having a uniform temperature;
- radiative transfer and heat transfer by conduction due to the collisions that the particles experience are negligible.

This set of assumptions allows us to compare the calculated numerical results with available experimental data. Relatively large particles are dealt with in the calculation reported in the present paper, since the capacity of the model to predict a possible enhancement of turbulence due to particles is sought. A first set of comparisons was made with the velocities and the turbulent quantities reported in the experimental study by Tsuji et al. [26]. This was done in order to study the influence of the source terms involved in the closure scheme. In particular, comparisons were performed between the results obtained with the classical formulation of the particle influence on the fluid turbulence and alternative solutions derived from the analysis by Crowe [9].

Then, the thermal characteristics were studied. Unfortunately, no experimental data are available for the temperature profiles of both phases. Consequently, validation of the thermal data may not be as complete as for the dynamics. A study of the sensitivity of our results to the modelling choices has however been done. Further comparisons based on suspension Nusselt numbers have been carried out.

### 3.1. Numerical handling

Considering the full set of equations to be solved, whatever the type of simulation chosen (Eulerian–Eulerian or Eulerian–Lagrangian), a classical iterative computation is carried out. This means that the final solution is sought following the successive steps listed below:

(i) search for a solution for the fluid phase in a one-phase flow configuration,
(ii) simulation of the dispersed phase in the corresponding continuous flow field,
(iii) search for an improved solution for the fluid phase, taking into account the influence of the dispersed phase,
(iv) simulation of the dispersed phase in the corrected flow field obtained after step (iii),
(v) repetition of steps (iii) and (iv) until no significant variation of the obtained results is observed.

Typically, in the results presented below, normalised residuals have been computed for each equation and convergence has been sought until all residuals have been found to be smaller than $10^{-5}$. A maximum of 60 iterations, including a repetition of steps (iii) and (iv) has

been computed in case of strong coupling between the two phases.

Since we are dealing with a thermally developing flow which is supposed to be dynamically fully developed, computation is performed once and for all for the dynamic part of the solution, then the same treatment is applied to heat transfer using an implicit scheme to treat the heat transfer in the axial direction. Consequently, in the Eulerian–Lagrangian solution, particles are first tracked in a given isothermal flow field, the whole dynamic problem is solved, dynamic characteristics (such as velocity, concentration) are stored, then the thermal part of the problem is solved. Particles are injected in the duct with a relative velocity equal to the free fall velocity and a uniform distribution. They are tracked along the duct up to the outlet, where their characteristics are stored so that they can be re-injected at the inlet in the next loop. The corresponding cyclic computation ensures that the analysed flow field corresponds to a dynamically fully developed flow, independent of inlet conditions. When entering the heated section, the remaining duct length then matches the experimental conditions given in the simulated experiments.

The source terms detailed in Table 2 are introduced in the formulation in step (iii). In order to ensure numerical stability of the whole solution, they are taken into account progressively, using an under-relaxation process. This is especially required in the case of the Eulerian–Lagrangian formulation, where the source terms are calculated at the end of step (iv) and then introduced in step (iii) in such a way that

$$S_{\mathrm{kf}}^{\text{present iteration introduced in step (iii)}} = 0.1\, S_{\mathrm{kf}}^{\text{previous iteration at the end of step (iv)}} + 0.9\, S_{\mathrm{kf}}^{\text{previous iteration used in step (iii)}} \tag{18}$$

The under-relaxation factor may even be fixed at a smaller value (0.05) in some difficult cases (when the coupling between the phases is strong, i.e. for large particles or when the loading ratio increases).

This numerical scheme is applied and care is taken as concerns the grid, which has been chosen in order to yield a very fine mesh near the wall (the requirement given by Myong and Kasagi [19] to allow the application of their low Reynolds model is that the position of the first node has to be at a distance from the wall lower than 0.6 wall units). Similarly the mesh is very fine at the entrance of the pipe (see Boulet et al. [16] for more details on the logarithmic way the mesh is stretched).

### 3.2. Velocity profiles

Let us examine a first set of comparisons of predicted velocity profiles with experimental data by Tsuji et al. [26]. The case of a pipe flow with a Reynolds number of 22 000, loaded with polystyrene beads (with diameter 501 μm and density 1030 kg/m$^3$) was addressed. In Fig. 1a, comparisons are given for a loading ratio of 1.3 between the experimental data (symbols) for the air flow and various calculation results obtained with our Eulerian–Eulerian model. The fluid velocity is normalised to that at the pipe axis $u_{\mathrm{f}}(r = 0)$.

One can note that the accuracy obviously requires a two-way solution even at a relatively moderate loading ratio. The formulation of the source term is also important but it is difficult to decide which model is the best, since model 2 is slightly better in the turbulent core, whereas its prediction of the near wall behaviour of the fluid velocity is not so good.

Fig. 1b illustrates the same subject with a larger loading ratio of 3.4. As expected, the two-way coupling effect, which can be estimated by comparing the thin line with one of the other curves, is greater. As the loading ratio is larger, the interaction terms have to be taken into account and better accuracy appears using the formulation of the source term following model 2. In Fig. 1c the same study is performed for smaller particles (with a diameter of 243 μm) and a loading ratio of 1.9. The influence of two-way coupling is still visible, but two-way coupling predictions tend to overestimate the particle influence. Model 2 seems to be less accurate in this case. It therefore seems difficult to derive a model which is accurate for a wide range of suspension properties, in particular the particle characteristic time or the loading ratio.

One reason for this misprediction of model 2 could be the fact that the estimation of the dissipation includes turbulence and interparticle distance effects whereas the distance to the wall could also become a key parameter in this near wall area. Another explanation could also come from the form of relation (17), which provides for the two-phase flow dissipation length a value smaller than both the interparticle spacing and the dissipation length for a one-phase flow, whereas an intermediate value might be more suitable.

### 3.3. Turbulence modulation

A complementary analysis has to be carried out on the fluid turbulence characteristics, owing to the strong influence of the turbulence which is expected on the thermal behaviour of the suspension. Using available experimental data by Tsuji et al. [26], a streamwise fluctuating velocity has been predicted using the various above-presented models. The case of a suspension with a Reynolds number of 22 000 loaded with 501 μm particles at a loading ratio of 1.3 is plotted on Fig. 2a. Again, the results are normalised to the velocity at the pipe axis. The previously observed trends are enforced. The two-way coupling effect on turbulence is more visible. The model using a classical formulation for the source terms

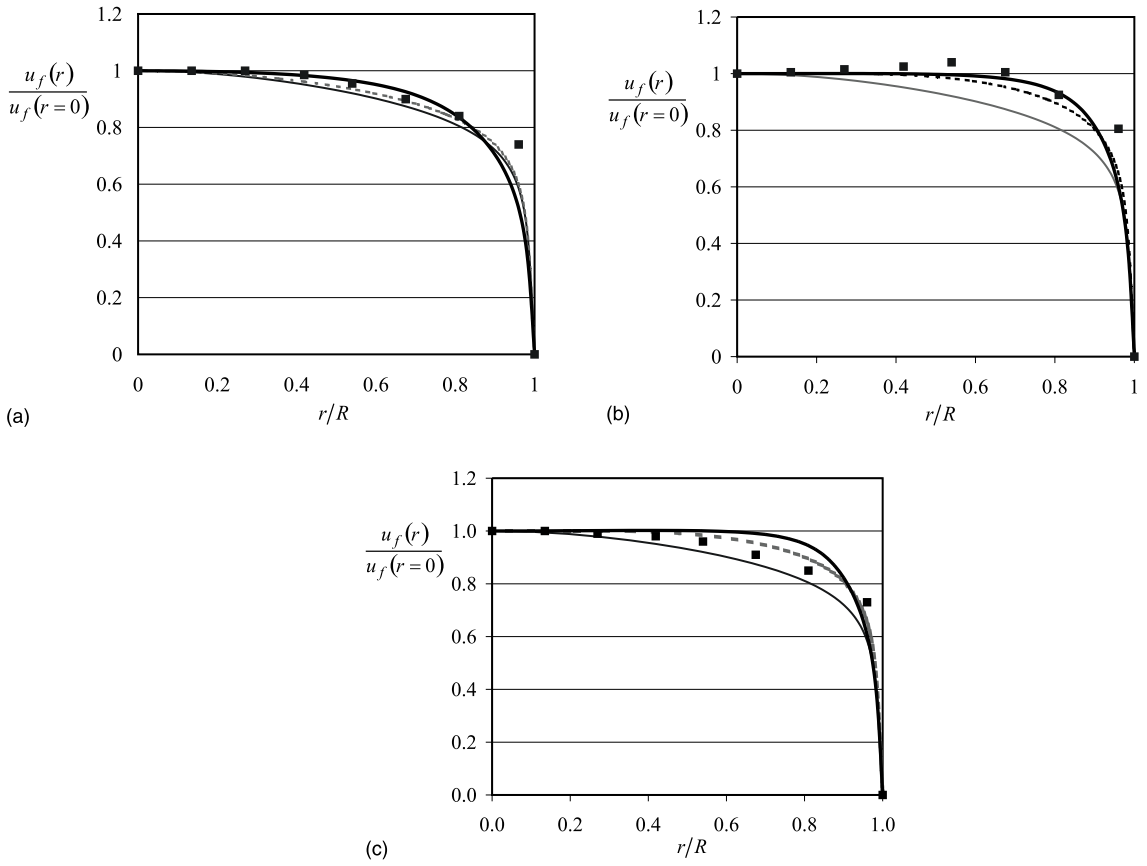


Fig. 1. Fluid velocity distribution as a function of radial position. The thin line corresponds to model 0, the dashed line is for model 1 and the thick continuous line is for model 2. Symbols are for experimental data by Tsuji et al. [26]. (a) $Re = 22000$, $d_p = 501$ μm, $m = 1.3$; (b) $Re = 22000$, $d_p = 501$ μm, $m = 3.4$; (c) $Re = 22000$, $d_p = 243$ μm, $m = 1.9$.

clearly under-predicts the real data, whereas the model following the Crowe formulation gives satisfactory results. In Fig. 2b the same conditions are applied for a larger loading ratio (3.4). Model 2 satisfactorily predicts the turbulence modulation, despite stronger coupling effects due to the larger loading ratio involved. As expected, a classical formulation is unable to predict turbulence enhancement. One may note however that the accuracy of the prediction obtained with model 2 is especially good near the pipe centre, whereas the profile is less accurate near the wall. This observation has to be associated with the previously noted misprediction of the near-wall velocity, which results in a bad estimation of the production term in the balance for $k_f$. The case of smaller particles (243 μm) is addressed on Fig. 2c. Again, the results are really satisfactory with the formulation of the source terms using model 2, despite a lower accuracy near the wall.

Considering this promising ability to predict turbulence enhancement when simulating a suspension loaded with large particles, complementary tests have been carried out. First of all, the possibility of using model 2 with an Eulerian–Lagrangian approach was investigated. Fig. 3 presents a comparison between the Eulerian–Eulerian simulation and the Eulerian–Lagrangian one, performed in the same conditions: $Re = 22000$, particle with diameter 501 μm and density 1030 kg/m$^3$, loading ratio 3.4. As can be seen, the source term modelling is suitable for the turbulence modulation, however the dispersed phase is simulated. In particular, the possibility of turbulence enhancement is confirmed by these results. A little discrepancy between the two methods appears though. One possible explanation could be that the particle Lagrangian tracking takes into account the lift force, whereas the Eulerian–Eulerian model does not. However, complementary computations performed by the authors, neglecting the lift force, gave no difference in the numerical results. Consequently, this can not be the true reason. A more likely explanation could lie in the discrepancies which have been observed between the concentration profiles obtained by the two methods. The Eulerian–Eulerian model gives a nearly flat profile

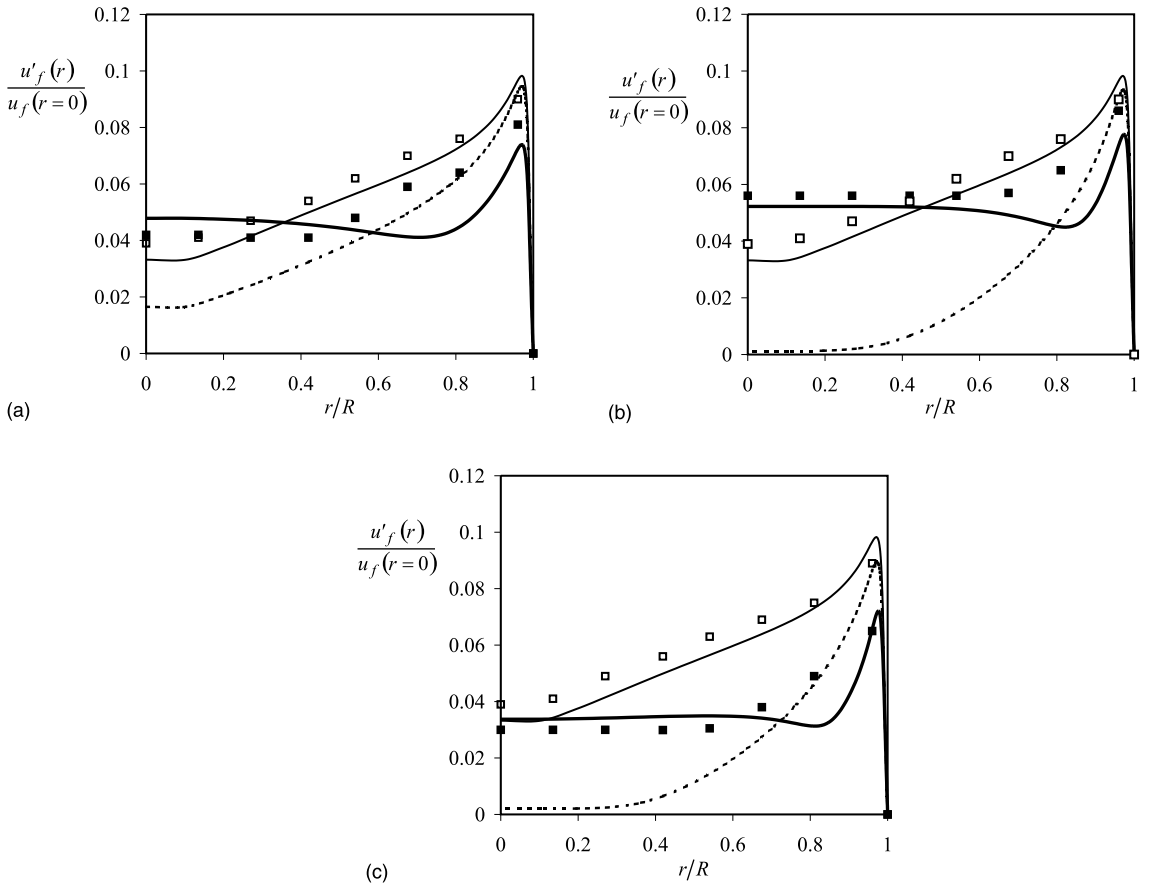


Fig. 2. Streamwise fluctuating velocity as a function of radial position. Same captions as in Fig. 1, with closed symbols corresponding to the experimental data by Tsuji et al. [26]. Open symbols are for experimental results obtained in the particle free flow. (a) $Re = 22000$, $d_p = 501$ μm, $m = 1.3$; (b) $Re = 22000$, $d_p = 501$ μm, $m = 3.4$; (c) $Re = 22000$, $d_p = 243$ μm, $m = 1.9$.

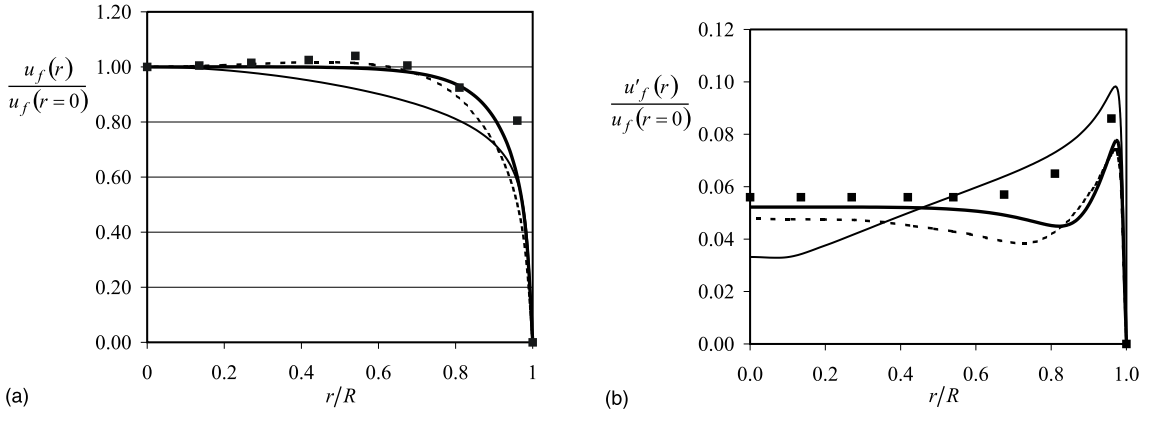


Fig. 3. Comparison between the Eulerian–Eulerian (thick solid line) and the Eulerian–Lagrangian (dashed line) formulation. Symbols are for experimental data (Tsuji et al. [26]). Case study: $Re = 22000$, $m = 3.4$, $d_p = 501$ μm. The thin solid line is for the simulation of the pure gas case. (a) Velocity profile; (b) streamwise fluctuating velocity.

whereas the Eulerian–Lagrangian one gives more deviations from the mean value. This difference certainly leads to slight discrepancies for the other calculated profiles as observed in Fig. 3b.

One remaining problem is the misprediction which has been noted near the wall. Supposing that the particular formulation of the dissipation could be invoked to explain this difficulty, a new model referred to as *model 3* was tested, using the formulation of $S_{kf}$ derived from the model by Crowe associated with a conventional form of the dissipation balance in a sort of hybrid model. The underlying idea is that a balance for the dissipation could be used, involving a classical form for the extra-dissipation term $S_{\varepsilon f}$ without any idea about the appropriate value of the constant $C_{\varepsilon 3}$. This possibility has been applied using an Eulerian–Eulerian formulation under the same conditions as in Fig. 3. Only little discrepancies have been observed for the mean velocity profiles when compared with Fig. 3a, for example. A stronger effect has been noticed for fluctuating velocities as reported in Fig. 4, however. In the classical formulation (model 1), the source terms usually have so little influence that a variation of $C_{\varepsilon 3}$ has nearly no effect on the final profile of the turbulent quantities. This is no longer the case with model 3, because of the strong influence of the extra-production, which causes significant enhancement of the turbulent kinetic energy. Consequently, adapting the extra-dissipation may produce a final result very close to experimental data as is obvious looking at the curve obtained for $C_{\varepsilon 3} = 1.85$ in Fig. 4a. Contrary to the results given by model 2, the profile is qualitatively well predicted and the near-wall behaviour is better than previously obtained. The apparent drawback of the method is the sensitivity of the result to $C_{\varepsilon 3}$, as is clear when looking at the discrepancy between the curves obtained with the values 1.8 and 1.85. Some tests have also indicated that any further increase in the constant $C_{\varepsilon 3}$ leads to numerical divergence, due to an overestimation of the extra-dissipation which causes the turbulent kinetic energy to take zero or even negative values. To illustrate the complexity of the determination of this constant, a second case is plotted in Fig. 4b, for a loading ratio of 3.4. Same comparisons are carried out. Despite the fact that a very accurate prediction seems to be achievable, a supplementary difficulty appears since the optimisation of the constant $C_{\varepsilon 3}$ provides a new value around 1.81. In some other cases (for example the case addressed in Figs. 1c and 2c), despite tests carried out by varying the value of $C_{\varepsilon 3}$, no satisfying agreement was obtained in the final results, the predicted profile being too far from the experimental prediction or numerical divergence occurring when further varying $C_{\varepsilon 3}$. Nevertheless, model 3 seems to be the best tool for predicting the dynamics of the flow, since it provides correct velocity and turbulence profiles, even near the wall. The sensitivity of the model to $C_{\varepsilon 3}$ has to be kept in mind however, since there is no way to a priori fix the exact value of this parameter, a value near 1.8 seeming to be a correct approximation in the tested cases. On the theoretical point of view, the question is also open on the actual definition of the dissipation. Usual assumption like "the size of the particle is smallest than the smallest eddy" is no more satisfied here, when taking into account the extra-production in the particle wake. Hence, may a classical $k$–$\varepsilon$ formulation yield a fully satisfactory tool to predict the fluid turbulence in a two-phase flow?

### 3.4. Consequence on the behaviour of non-isothermal flows

Let us now deal with the thermal part of the numerical simulation. In order to allow comparisons of the numerical results with available experimental data, the Nusselt numbers are predicted to characterise the heat exchanges between the wall and the suspension. Let us therefore investigate the modification of the heat transfer between the flow and the pipe wall, by calculating a suspension Nusselt number as follows:

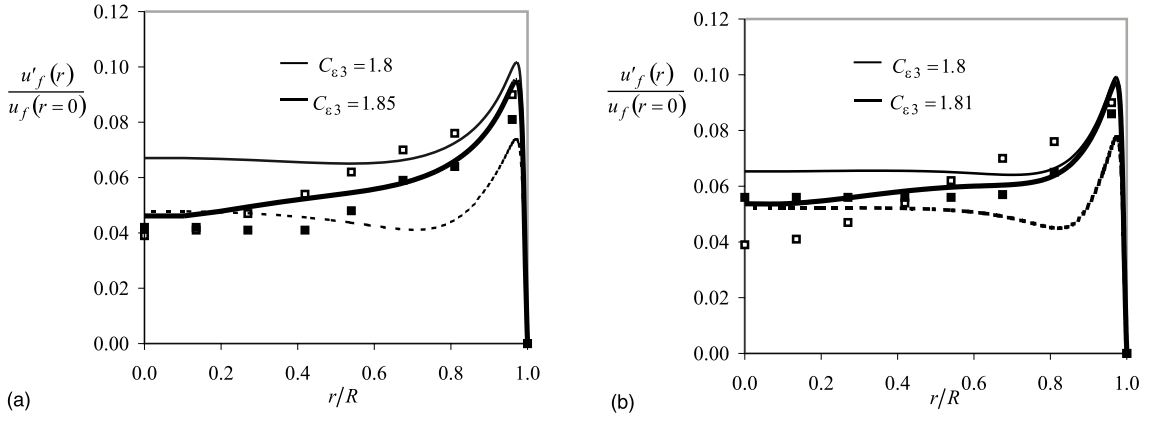


Fig. 4. Streamwise fluctuating velocity predicted using model 3. Two values of $C_{\varepsilon 3}$ have been used. The dashed line is for the previously presented model 2, for comparison. (a) $Re = 22000$, $d_p = 501$ μm, $m = 1.3$; (b) $Re = 22000$, $d_p = 501$ μm, $m = 3.4$.

$$Nu_s = \frac{DQ_w}{\lambda_f(\theta_w - \theta_m)} \tag{19}$$

where $D$ is the pipe diameter, $Q_w$ is the heat flux at wall, $\theta_w$ is the wall temperature and $\theta_m$ is the bulk mean temperature given by:

$$\theta_m = \frac{2\pi \int_0^{D/2}(1-\alpha)\rho_f c_{pf} u_f \theta_f r\,dr + 2\pi \int_0^{D/2} \alpha\rho_p c_{pp} u_p \theta_p r\,dr}{q_{mf} c_{pf} + q_{mp} c_{pp}} \tag{20}$$

where $q_{mf}$ and $q_{mp}$ are the mass flux of the fluid phase and the solid phase, respectively.

A first set of comparisons was provided with the experimental data by Jepson et al. [27], corresponding to the following conditions:

- thermal boundary condition: constant wall heat flux,
- pipe diameter: 0.0381 mm,
- heated section length: 3.65 m,
- suspension loaded with sand particles with mean diameter 500 μm,
- Reynolds number around 30 900 or 46 500.

Fig. 5a summarises the possible comparisons between predictions and experimental data, the suspension Nusselt number being divided by the value computed for the pure gas flow ($Nu_0$). Various tests have been carried out using the different models previously referred to as models 1, 2 and 3, in applying the conditions given by Jepson et al. However, the inability of models 1 and 2 to produce accurate results is observed. In accordance with the previous paragraph, this inability is attributed to the failure of model 1 in predicting any turbulence enhancement on one hand, and to the misprediction of the near-wall turbulence level produced by model 2 on the other. Hence, all the computations presented hereafter have been performed using model 3 with a value of 1.8 for the constant $C_{\varepsilon 3}$, keeping in mind the numerical problems discussed at the end of the previous paragraph.

The agreement between numerical and experimental data is slightly better upon using the Eulerian–Eulerian solution. Although qualitatively good, the Eulerian–Lagrangian prediction overestimates the Nusselt number (as another example will show it later in Fig. 7), which has not been explained as yet.

Things are more complicated when simulating suspensions loaded with smaller particles. The same conditions are used in Fig. 6 except for the particle diameter which is now equal to 250 μm (only Eulerian–Eulerian results are presented). In this case, numerical convergence was very difficult to achieve unless turbulence source terms were forced to 0 in the region very near to the wall. This is not so surprising, considering that various damping functions are used in the model, whereas none are applied for the source term simulating the particle–turbulence interactions. Upon performing numerous tests, a condition of damping the turbulence source term at a distance less than a particle diameter was found to provide numerical predictions with the best agreement with experimental data. This idea arose from the observation of sharp variations of the turbulence source terms in the near wall layer, whereas the turbulence level is known to be very small in this region. Of course, this is not a satisfactory solution despite the apparent accuracy of the prediction as can be observed

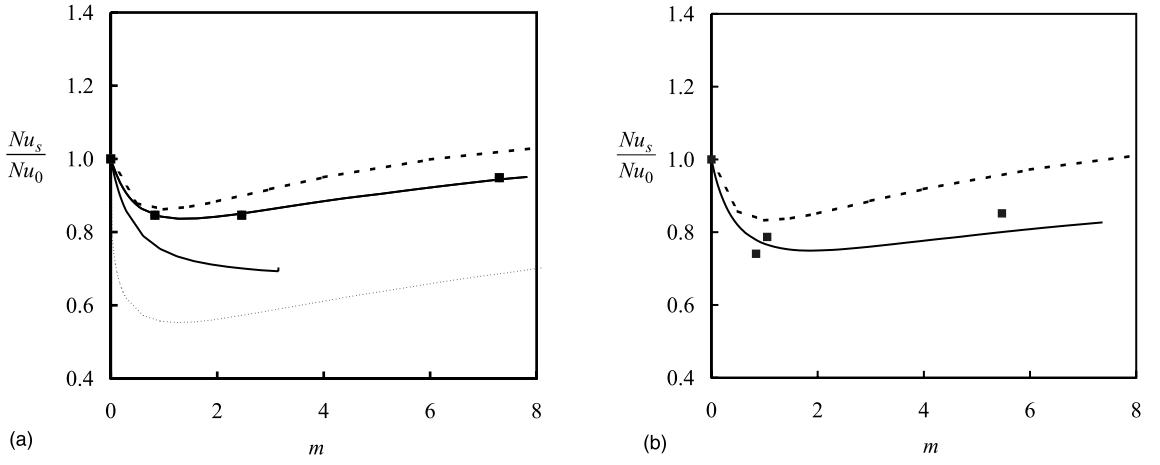


Fig. 5. Simulation of Nusselt number variation as a function of loading ratio. The suspension Nusselt number is normalised by the particle free flow Nusselt value. Symbols are for experimental data by Jepson et al. [27]. The thick solid line is for the Eulerian–Eulerian model. The thick dashed line is for the Eulerian–Lagrangian simulation. In (a), the thin solid line and the thin dashed line correspond to Eulerian–Eulerian results obtained with models 1 and 2 respectively. (a) $Re = 30\,900$, sand particles with diameter $d_p = 500$ μm; (b) $Re = 46\,500$, sand particles with diameter $d_p = 500$ μm.

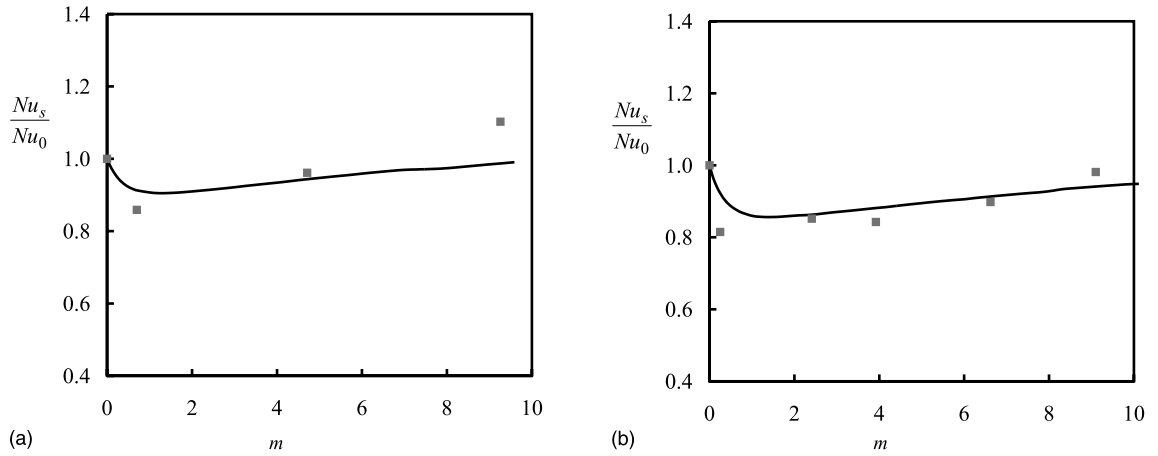


Fig. 6. Simulation of Nusselt number variation as a function of loading ratio (Eulerian–Eulerian results only). Same caption as for Fig. 5. (a) $Re = 30\,900$, sand particles with diameter $d_p = 250$ μm; (b) $Re = 46\,500$, sand particles with diameter $d_p = 250$ μm.

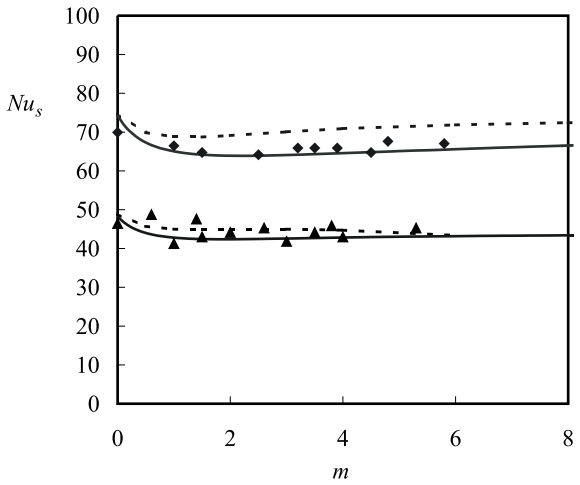


Fig. 7. Simulation of Nusselt number variation as a function of loading ratio. Symbols are Farbar and Depew's experiments [28]. Same captions as for Fig. 5. Case study: $Re = 15\,300$ and 26 500, suspension loaded with glass particles, $d_p = 200$ μm.

in Fig. 6 and more especially in Fig. 7 as seen below. One may add that this damping of the turbulence source term in the near-wall region has been observed to have very little influence on the results previously presented for larger particles (in Fig. 5). A more general solution is sought however, such as a new damping function for $C_{\varepsilon 3}$ for example. The agreement between numerical and experimental results is good, even if slight discrepancies may be observed at largest loading ratios, indicating the difficulty to obtain an accurate model for a wide range of suspension characteristics. One has to keep in mind that all constants and functions involved in the simulation come from the field of one-phase flow applications, whereas adaptation to two-phase flows with various characteristics could be necessary. This implies a very complicated optimisation problem.

A second set of comparisons concerns the simulation of Farbar and Depew' experiments [28]. The conditions are as follows:

- thermal boundary condition: constant wall temperature,
- pipe diameter: 0.0175 mm,
- heated section length: 0.84 m,
- suspension loaded with glass particles with diameter 200 μm,
- Reynolds number equal to 15 300 or 26 500.

In order to be close to the experimental data, the Nusselt number calculation has been adapted here. Following the indication given by Farbar and Depew, the suspension Nusselt number is now computed using a logarithmic temperature difference defined as

$$\Delta T_{\mathrm{LM}} = \frac{(\theta_{\mathrm{w}} - \theta_{\mathrm{m_{outlet}}}) - (\theta_{\mathrm{w}} - \theta_{\mathrm{m_{inlet}}})}{\ln \dfrac{(\theta_{\mathrm{w}} - \theta_{\mathrm{m_{outlet}}})}{(\theta_{\mathrm{w}} - \theta_{\mathrm{m_{inlet}}})}} \tag{21}$$

where $\theta_{\mathrm{m_{inlet}}}$ and $\theta_{\mathrm{m_{outlet}}}$ stand for the bulk mean temperature at the inlet and the outlet of the heated section, respectively.

This allows the calculation of the wall heat flux as

$$Q_{\mathrm{w}} = (q_{mf} c_{\mathrm{pf}} + q_{m\mathrm{p}} c_{\mathrm{pp}})(\theta_{\mathrm{m_{outlet}}} - \theta_{\mathrm{m_{inlet}}}) = h_{\mathrm{s}} S_{\mathrm{w}} \Delta T_{\mathrm{LM}} \tag{22}$$

where $h_{\mathrm{s}}$ designates the heat transfer coefficient between the wall and the suspension and $S_{\mathrm{w}}$ is the heated pipe surface.

Finally the suspension Nusselt number is

$$Nu_s = \frac{h_s D}{\lambda_f} \tag{23}$$

Fig. 7 presents various simulations using the above-mentioned model 3. Here again, turbulence source terms have to be neglected in the near-wall layer as previously mentioned. Provided this damping is done, numerical results are very close to the experimental ones.

Our conclusion is that the ability to simulate any turbulence enhancement has been confirmed, but the accuracy of the heat transfer prediction requires more care since the simulation of the near-wall area is very important.

## 4. Concluding remarks

In addressing the issue of numerical prediction of non-isothermal gas–solid flows, special care must be taken concerning the possible influence of the model used for particle–turbulence interactions. The formulation of the source term for the fluid turbulent kinetic energy according to the analysis by Crowe [9] has been observed to yield very interesting results, in so far as turbulence enhancement due to large particles could be predicted. Numerical computations were found to be optimal when solving a complete balance for the dissipation (analogous to the one usually solved in standard $k$–$\varepsilon$ models), rather than when using an algebraic approximation for the prediction of the dissipation. A fully satisfactory solution on both theoretical and numerical points of view has still to be sought, however. Finally, the implication of this turbulence modulation modelling has been observed on heat transfer prediction. Owing to the lack of accuracy of the models tested for the near wall dynamics, numerical predictions are possible provided damping of the particle–turbulence interactions is performed very close to the wall. Corresponding developments are now needed to improve the quality of the predictions in this region. In particular, more information is required about the so-called $C_{\varepsilon 3}$ constant, which probably is not strictly constant but rather a function of various factors like the particle Reynolds number, the solid volume fraction or the dimensionless wall distance.

## References


[1] S. Elghobashi, On predicting particle-laden turbulent flows, Appl. Sci. Res. 52 (1994) 309–329.

[2] R.A. Gore, C.T. Crowe, Effect of particle size on modulating turbulent intensity, Int. J. Multiphase Flow 15 (2) (1989) 279–285.

[3] A. Berlemont, P. Desjonqueres, G. Gouesbet, Particle Lagrangian simulation in turbulent flows, Int. J. Multiphase Flow 16 (1) (1990) 19–34.

[4] P. Desjonqueres, Modélisation Lagrangienne du comportement de particules discrétes en écoulement turbulent, Ph.D. Thesis, Rouen, France, 1987.

[5] M.Y. Louge, J.M. Yusof, J.T. Jenkins, The role of particle collisions in pneumatic transport, J. Fluid Mech. 231 (1991) 345–359.

[6] J. He, O. Simonin, Numerical modelling of dilute gas–solid turbulent flows in vertical channel, EDF Report HE-44/94/021/A (Direction des Etudes et Recherches, EDF) (1994).

[7] Z. Yuan, E.E. Michaelides, Turbulence modulation in particulate flows a theoretical approach, Int. J. Multiphase Flow 18 (5) (1992) 779–785.

[8] L.P. Yarin, G. Hetsroni, Turbulence intensity in dilute two-phase flows-3: the particles–turbulence interaction in dilute two-phase flow, Int. J. Multiphase Flow 20 (1) (1994) 27–44.

[9] C.T. Crowe, On models for turbulence modulation in fluid-particle flows, Int. J. Multiphase Flow 26 (5) (2000) 719–727.

[10] C.T. Crowe, M. Sommerfeld, Y. Tsuji, Multiphase Flows with Droplets and Particles, CRC Press, Boca Raton, 1998.

[11] G.J. Hwang, H.H. Shen, Fluctuation energy equations for turbulent fluid–solid flows, Int. J. Multiphase Flow 19 (5) (1993) 887–895.

[12] I. Kataoka, A. Serizawa, Basic equations of turbulence in gas–liquid two-phase flow, Int. J. Multiphase Flow 15 (5) (1989) 843–855.

[13] L.M. Liljegren, Ensemble-averaged equations of a particulate mixture, J. Fluid Engng. 119 (1997) 428–434.

[14] S. Lain, D. Broder, M. Sommerfeld, Experimental and numerical studies of the hydrodynamics in a bubble column, Chem. Engng. Sci. 54 (1999) 4913–4920.

[15] P. Boulet, B. Oesterlé, A. Tanière, Prediction of heat transfer in a turbulent gas–solid pipe flow using a two-fluid model, Particul. Sci. Technol. 17 (4) (1999) 253–267.

[16] P. Boulet, S. Moissette, R. Andreux, B. Oesterlé, Test of an Eulerian–Lagrangian simulation of wall heat transfer in a gas–solid pipe flow, Int. J. Heat Fluid Flow 21 (2000) 381–387.

[17] J. Sun, M.M. Chen, A theoretical analysis of heat transfer due to particle impact, Int. J. Heat Mass Transfer 31 (5) (1988) 969–975.

[18] M. Rokni, B. Sunden, Improved modeling of turbulent forced convective heat transfer in straight ducts, Trans. ASME—J. Heat Transfer 121 (1999) 712–719.

[19] H.K. Myong, N. Kasagi, A new approach to the improvement of $k$–$\varepsilon$ turbulence model for wall-bounded shear flows, JSME Int. J., Series II 33 (1) (1990) 63–72.

[20] C.M. Hrenya, E.J. Bolio, D. Chakrabarti, J.L. Sinclair, Comparison of low Reynolds number $k$–$\varepsilon$ turbulence models in predicting fully developed pipe flow, Chem. Engng. Sci. 50 (12) (1995) 1923–1941.

[21] C. Hrenya, S. Miller, T. Mallo, J. Sinclair, Comparison of low Reynolds number $k$–$\varepsilon$ turbulence models in predicting heat transfer rates for pipe flow, Int. J. Heat Mass Transfer 41 (11) (1998) 1543–1547.

[22] M. Rokni, T.B. Gatski, Predicting turbulent flow and heat transfer in 3D ducts using an EASM, in: Y. Nagano, K. Hanjalic, T. Tsuji (Eds.), Proceedings of the 3rd

International Symposium on Turbulence, Heat and Mass Transfer, Aichi Shuppan, Japan, 2000, pp. 357–364.

[23] E.J. Bolio, J.A. Yasuna, J.L. Sinclair, Dilute turbulent gas–solid flow in risers with particle–particle interactions, AIChE J. 41 (6) (1995) 1375–1388.

[24] M. Sommerfeld, Modelling of particle–wall collisions in confined gas–particle flows, Int. J. Multiphase Flow 18 (1992) 905–926.

[25] S. Moissette, B. Oesterlé, P. Boulet, Simulation of particle temperature fluctuations in Eulerian–Lagrangian predictions of heat transfer in a turbulent gas–solid pipe flow, in: Proceedings of the ASME FEDSM 2000, Paper 11143, 2000.

[26] Y. Tsuji, Y. Morikawa, H. Shiomi, LDV measurements of an air–solid two-phase flow in a vertical pipe, J. Fluid Mech. 139 (1984) 417–434.

[27] G. Jepson, A. Poll, W. Smith, Heat transfer from gas to wall in a gas/solids transport line, Trans. Instn. Chem. Engrs. 41 (1963) 207–211.

[28] L. Farbar, C.A. Depew, Heat transfer effects to gas–solids mixtures using solid spherical particles of uniform size, I & EC Fundamentals 2 (2) (1963) 130–135.